

Georgia Tech Sponsored Research

Project	E-20-F35	
Project director	Frost	James
Research unit	CEE	
Title	Paleoseismology and Paleoliquifaction	
Project date	9/30/2000	

21

E-20-F35
#1

Progress Report

Contributions to
Project # SG-3 – Paleoseismology and Paleoliquefaction

Prepared by
Chien-Tai Yang and J. David Frost
The Georgia Institute of Technology

Submitted to
NSF Mid-America Earthquake Center

January, 2001

Laboratory Investigation of Sand Blows

Introduction

This report summarizes the findings of a one-year study conducted at the Georgia Institute of Technology with partial support from the NSF Mid-America Earthquake (MAE) Center. The work was undertaken as a contribution to a larger multi-year study being performed by other MAE researchers into paleoseismology and paleoliquefaction. Further work is being conducted by the investigators in addition to what was accomplished during the period for which MAE support was provided. This scope of this additional work is noted at the end of this report but is not presented here since it is still in progress. The investigators anticipate presenting this work at a later date even though it is not being supported by MAE/NSF.

During the one-year MAE project, the investigators undertook to develop apparatus that would allow sand blows to be generated and visually observed in the laboratory. Although the exact procedure used to generate the sand blows (upward flow of water induced by a hydraulic source beneath the base of a two-dimensional apparatus) differs from what is understood to occur under field conditions (upward flow of water due to pore pressures gradients generated by collapse of pore structures as a result of dynamic loading), the resulting genesis and evolution of sand blows observed in the laboratory is believed to provide interesting insight into a number of aspects of the mechanisms of sand blows. Following some preliminary "proof of concept" tests, apparatus was developed as part of this study to allow the characteristics of sand blows to be evaluated under controlled conditions in the laboratory. Using this apparatus, a total of fourteen tests were performed to obtain a better understanding of sand blows and how they can be influenced by the microstructure of the subsurface materials. These tests were used to evaluate the influence of sand type on the observed response, to understand the effect of different flow types on the sand blow characteristics, to assess the role of defects on sand blow genesis and to investigate the effect of depositional stratigraphy on the response of the sand.

Apparatus Design

Sand blows are generally formed by water venting to the ground surface from zones of high pore pressure generated at shallow depth by the compaction of granular soils during seismic shaking. Accordingly, one of the main factors that influences whether sand blows will form is the permeability of the subsurface soils. In this respect, there are two factors to be considered that can influence the degree to which sand blows may form. Firstly, there needs to be a zone of soil that is susceptible to collapse so that the necessary “reservoir” of elevated pore pressure is available. Secondly, if an overlying confining layer is present, this can contribute to a more rapid generation of the zone of higher pore pressure and thus more dramatic upward flow of fluid. If the desire is to induce sand blows in the laboratory, it is thus important to select soil with a suitable permeability. If the coefficient of permeability of the selected soil is large, it may be difficult to observe the phenomena of blows in the lab. On the other hand, if the coefficient of permeability of the selected soil is relatively small, voids at the boundary of the apparatus may govern the behavior of the blows. In these cases, partial blows may be generated at the side of the apparatus because the boundary of the apparatus is rigid (not flexible) and thus the permeability along the boundary may be higher than inside the soil.

At the stage of designing the apparatus, two viewpoints were considered for investigating sand blows. The first one was to view the apparatus as one unit (square) of a flow net. In this case, the two vertical boundaries of the apparatus (ends) were considered as flow lines. The bottom and the top of the sand were equipotential lines. In this case, water pressure applied uniformly across the bottom of the tank could be used to simulate homogenous flow. In the second case, the apparatus was used to visualize the entire flow region (net). Concentrated water flow from a central point at the bottom of the tank was considered to more closely simulate how the flow of water in the subsurface could produce sand blows. The entire process of sand blow growth could be observed from the front of the two-dimensional apparatus.

Stratigraphic variations within the sand were also expected to play an important role in the process of sand blow formation/evolution. Accordingly, different stratigraphic structures were formed during sample preparation. Tests conducted on specimens with different inherent stratigraphic conditions were expected to provide insight into what can occur when the fluid flow in sand blows meets an inclined, synclinal or anticlinal stratigraphic feature.

Apparatus

The custom apparatus designed and built during this study included a pluviation apparatus to enable specimens to be reliably constructed using different sands to a desired initial condition (density and stratigraphy). Details of the apparatus are shown in Figure 1. In addition, a two-dimensional flow tank with plexiglass front and rear panels was designed and fabricated. The 5 cm wide tank measured approximately 60 by 60 cm. This device enabled the initial and evolving conditions within the soil to be visually observed and recorded. Details of the apparatus are shown in Figure 2.

Results

Table 1 summarizes the configurations of the 14 tests conducted. The key observations during each of the tests are summarized below.

Table 1: Configurations of Laboratory Tests

Test Number	Type of Soil	Flow Type	Stratigraphy	Initial Condition
I	Ottawa 20-30 Sand	Homogenous	Horizontal	Dry
II	ASTM Graded Sand	Homogenous	Horizontal	Dry
III	ASTM F-70	Homogenous	Horizontal	Dry
IV	ASTM F-70	Concentrated	Horizontal	Dry
V	ASTM F-70	Homogenous	Inclined	Dry
VI	ASTM F-70	Concentrated	Inclined	Dry
VII	ASTM F-70	Homogenous	Synclinal	Dry
VIII	ASTM F-70	Concentrated	Synclinal	Dry
IX	ASTM F-70	Homogenous	Anticlinal	Dry
X	ASTM F-70	Concentrated	Anticlinal	Dry
XI	ASTM F-70	Concentrated	Inclined	Wet
XII	Kaolinite	Homogenous	Horizontal	Dry
XIII	ASTM F-70	Homogenous	Horizontal	Wet
XIV	ASTM F-70	Concentrated	Horizontal	Wet

TEST I: (Shown in Figure 3)

Type of Soil	Flow Type	Stratigraphy	Initial Condition
Ottawa 20-30 Sand	Homogenous	Horizontal	Dry

This test involved a uniform flow being applied to the base of an Ottawa 20-30 sand specimen. As the water level reached the top of the sand, a sand blow was generated where the disturbance of the surface can be observed (Figure 3d). The area affected by the sand blow could be observed more clearly after the water

was allowed to drain out at the end of the test (Figure 3h). The sand within the blow neck had a higher permeability (larger porosity) as confirmed by the fact that the water in this zone drained out more quickly than in the other zones at the end of the test. This test was also used to investigate whether a localized defect would influence the behavior. To create a defect, a metal rod was inserted vertically near the left boundary of the tank and can be seen in all the photos. The presence of this rod did not have a significant effect in this experiment.

TEST II: (Shown in Figure 4)

Type of Soil	Flow Type	Stratigraphy	Initial Condition
ASTM Graded Sand	Homogenous	Horizontal	Dry

This test was similar to the first test except that ASTM graded sand was used. The inherent stratigraphic structure in the sand, although not readily evident immediately after sample preparation, became very clear upon wetting as seen by several dry seams (Figure 4c) which remained after the homogenous flow had been applied. When the wetting surface increased to a height of about 10 cm above the bottom of the tank, the sand was lifted along one of these “dry” seams which seemed to suggest that even the marginally lower permeability associated with the unsaturated zone was sufficient to cause it to act like a confining layer. The lifting motion evolved from being initially global to a more local phenomenon later in the test.

TEST III: (Shown in Figure 5)

Type of Soil	Flow Type	Stratigraphy	Initial Condition
ASTM F-70	Homogenous	Horizontal	Dry

This test was similar to the first two tests and was conducted to evaluate the effect of homogenous flow in ASTM F-70 sand and evaluate whether a local defect would affect this test configuration. Again, a thin metal rod inserted vertically near the left boundary was used to simulate a defect. Early in this test, the entire sand block started to be lifted upward (Figure 5b). The subsequent photos show that the sand block continues to be lifted upward and the block becomes like an arch. This arching response is attributed to the shear forces at the ends of the apparatus. The sand block was lifted upward a total of about 6 to 8 cm. A number of phenomena can be observed in this test. Firstly, the thin rod becomes a weak point of the sand

block (Figure 5d). The sand block can be seen to begin collapsing at the location of the thin rod. Secondly, the sand at the underside of the block starts to “unravel”. Thirdly, the arching movement generates two “normal faults” at the surface near the center of the sand block and another “reverse fault” towards the right end. Finally, the wetting front can also be seen to be arched thus it is clearly influenced by the depositional structure.

TEST IV: (Shown in Figure 6)

Type of Soil	Flow Type	Stratigraphy	Initial Condition
ASTM F-70	Concentrated	Horizontal	Dry

This test configuration differed from Test III in that a concentrated water source was used. The propagation of the water is very clear and the wetting front is like a semi-circle in the early stages (Figure 6a). The structure of the sand affects the propagation of the water. The horizontal propagation of the water is faster than the vertical one because of the effects of structure and gravity. A circular hole is initially generated by the high water head (Figure 6b). The hole becomes larger as more water flows into the system. A heave is generated at the surface near the center and two “reverse faults” are formed between the edges of the hole and the boundary of the heave (Figure 6c). These “reverse faults” are the weak points in the stratigraphy and the water attempts to release the high pressure through these faults. The shape of the hole becomes irregular and continues to increase its size (Figure 6d). The sand above the hole is deformed and pushed upward by the deforming hole. The water attempts to find a way to release high pressure and continues to deform the overlying sand. Due to the deformation, the overlying sand produces new weak points or shortcuts to the surface. Finally, a sand blow is generated at the center (Figure 6h).

TEST V: (Shown in Figure 7)

Type of Soil	Flow Type	Stratigraphy	Initial Condition
ASTM F-70	Homogenous	Inclined	Dry

The capillary effect due to the inclined structure of the sand can be seen in the early stages of this test (Figure 7a). The propagation speed is a little faster parallel to than it is perpendicular to the sand structure. The wetting surface at the right side of the sand tank also rises a little faster than at the left side of the sand tank. The structure clearly affects the manner in which the water propagates in the system. At later stages

in the test, the sand is lifted as a block (Figure 6d). The right side of the sand tank is lifted higher than the left side. The pattern of erosion (dropping of sand from the bottom of the sand block) is strongly influenced by the sand structure (Figure 6f). Finally, the erosion parallel to the stratigraphic structure reaches the surface (Figure 6h).

TEST VI: (Shown in Figure 8)

Type of Soil	Flow Type	Stratigraphy	Initial Condition
ASTM F-70	Concentrated	Inclined	Dry

The effect of the structure can also be readily seen when a concentrated water source is used with an inclined stratigraphy. The shape of the wetting front is not semi-circular because of the effect of structure and gravity. A hole with an irregular disc shape is generated and it appears that the shape of the hole is influenced by the presence of the inclined layer. The size of the disc-shaped hole grows as the test proceeds. When the void approaches the surface, it changes orientation and develops parallel to the structure.

TEST VII: (Shown in Figure 9)

Type of Soil	Flow Type	Stratigraphy	Initial Condition
ASTM F-70	Homogenous	Synclinal	Dry

The wetting front does not expand uniformly because of the effect of the synclinal structure. The propagation of the water at the center of the syncline is faster than at the two edges. After the sand block is lifted (Figure 9c), it gradually becomes like an arch and raveling occurs within the void almost perpendicular to the structure. As the test proceeds, the arching diminishes the syncline and the structure becomes more horizontal. When the large void nears the sand surface, it exits to the surface perpendicular to the structure.

TEST VIII: (Shown in Figure 10)

Type of Soil	Flow Type	Stratigraphy	Initial Condition
ASTM F-70	Concentrated	Synclinal	Dry

This test also shows that the propagation of the wetting front due to a concentrated source is faster at the center than at the two wings of the syncline (Figure 10b). Two defects develop near the bottom of the tank (Figure 10c). Two “reverse faults” are generated by the deformation of the hole and a heave is seen at the surface near the center (Figure 10d). Two fissures attempt to evolve parallel to the structure from the top of the hole (Figure 10f). The hole becomes larger but this structure seems to be more stable than in other cases as evidenced by the fact that no blow exits at the surface despite the large volume of the material in a slurry condition (Figure 10h).

TEST IX: (Shown in Figure 11)

Type of Soil	Flow Type	Stratigraphy	Initial Condition
ASTM F-70	Homogenous	Anticlinal	Dry

The phenomena in this test are similar to those observed in the other tests. The sand is lifted as a block (Figure 11c). The propagation of the wetting front is slower at the center than at the two wings of the anticline. Unravelling of the soil at the bottom of the block occurs parallel to the structure at the left side. A sand blow exits to the surface perpendicular to the structure near the end of the test (Figure 11h).

TEST X: (Shown in Figure 12)

Type of Soil	Flow Type	Stratigraphy	Initial Condition
ASTM F-70	Concentrated	Anticlinal	Dry

An elliptical hole is located at the crest of the anticline and does not change shape during the deformation. The area affected by the deformation of the hole is much smaller than in the other cases. Two “reverse faults” occur directly above the hole and a small heave is noted at the surface near the center (Figure 12d). These weak points facilitate the propagation of the hole and a sand blow reaches the surface. In this case, the zone affected (the loose sand area) is smaller than in the other tests with a concentrated water source (Tests IV, VI, and VIII). It can be seen that this type of the structure focuses the growth of the sand blow to the crest and leads to a more rapid growth.

TEST XI: (Shown in Figure 13)

Type of Soil	Flow Type	Stratigraphy	Initial Condition
--------------	-----------	--------------	-------------------

ASTM F-70	Homogenous	Inclined	Wet
-----------	------------	----------	-----

The configuration for this test was the same as in Test V except that the test was conducted with the sand initially wet. This was accomplished by first adding water from the top at a very slow rate before the water was allowed to enter from the bottom. The propagation direction of the hole is perpendicular to the structure. The propagation of the hole kept the same orientation until it reached the side of the apparatus. Then a sand blow was created at the side of the apparatus. As flows continued, a second sand blow was generated near the first one but the path to the surface was shorter. Finally, a third sand blow was generated and followed a near vertical path to the surface.

TEST XII: (Shown in Figure 14)

Type of Soil	Flow Type	Stratigraphy	Initial Condition
Kaolinite	Homogenous	Horizontal	Dry

This test was conducted using kaolinite to investigate the effect of low permeability soils on the evolution of sand blows. Even though a very low water flow rate was used, a horizontal crack was created early in the test (Figure 14a). The water escaped from the side of the apparatus. The permeability of the pore at the boundary of apparatus and not the permeability of kaolinite governed this test.

TEST XIII: (Shown in Figure 15)

Type of Soil	Flow Type	Stratigraphy	Initial Condition
ASTM F-70	Homogenous	Horizontal	Wet

The genesis and evolution of a sand blow in saturated sand was not significantly different to what was observed with initially dry sand with the exception that the process in the saturated sand was much faster. Since the voids in the saturated sand were already occupied by water, the process of sand blow growth and evolution was much faster.

TEST XIV: (Shown in Figure 16)

Type of Soil	Flow Type	Stratigraphy	Initial Condition
ASTM F-70	Concentrated	Horizontal	Wet

After the water flow was initiated, the combination of the capillary force and the uplift force led to the generation of some voids in the soil (Figure 16b). The number of the voids in the sand structure increased as the test progressed. These voids provided weak points along which the sand blows evolved.

Discussion

The tests summarized in the preceding section provided some interesting insight into the mechanisms that can influence the genesis/evolution of sand blows. While clearly the scale tests presented herein have some limitations (similitude issues), they are believed to provide valuable evidence of the influence of material index and structural properties on the genesis/evolution of sand blows as summarized below.

Effect of material permeability: The tests performed in this study show that for a given flow rate sand blows can be more readily induced in the laboratory with lower permeability sands. While for higher permeability materials it is still possible to generate sand blows, the fluid flow rate is so large that observing the various phases of the process becomes more difficult. With somewhat lower permeability materials, all aspects of the process can be readily examined. Further, for lower permeability sands, it was easier to demonstrate the influence of a “defect” in the subsurface in terms of controlling where the blow occurred. Based on the tests described herein, it was clear that a minor defect could play a significant role in determining where a sand blow may occur. As the permeability of the material is reduced further (e.g. test with Kaolinite), other boundary factors enter the picture and can diminish the ability to control the genesis/evolution of sand blows.

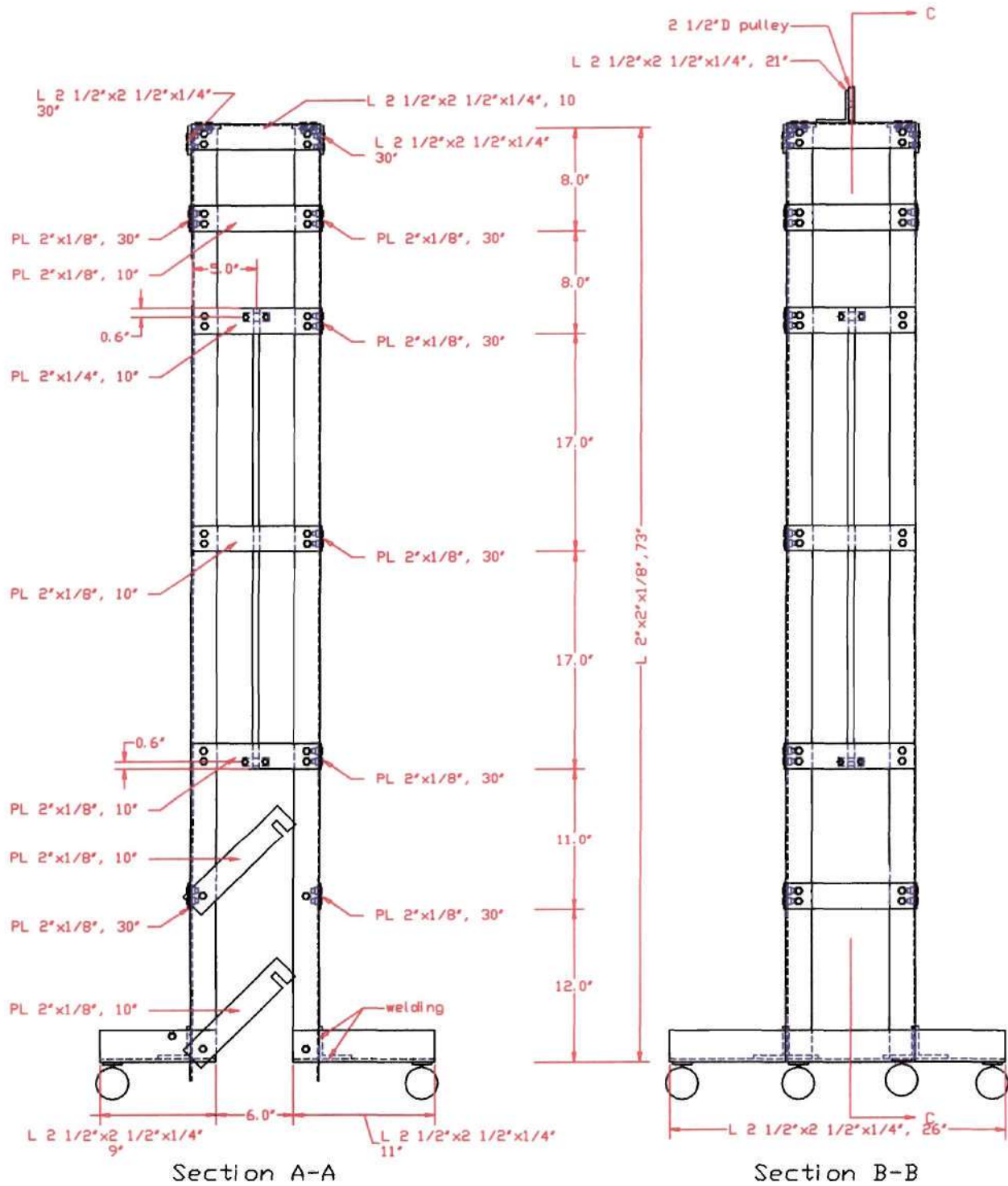
Effect of inherent structure: Structure induced during the deposition of the soil has a dramatic influence on how sand blows evolve. The structure can effect how the deposit “ravels” internally at a microscale as well as how it behaves from a macroscale perspective as a “block” of material subjected to a boundary water pressure. The different inherent structures examined in this study showed significant variations in how a subsurface environment could influence the rate and extent of sand blow evolution. It was also evident that in the absence of a defect, the rate at which a sand blow evolved and migrated towards the surface was very dependent on the inherent structure of the deposit.

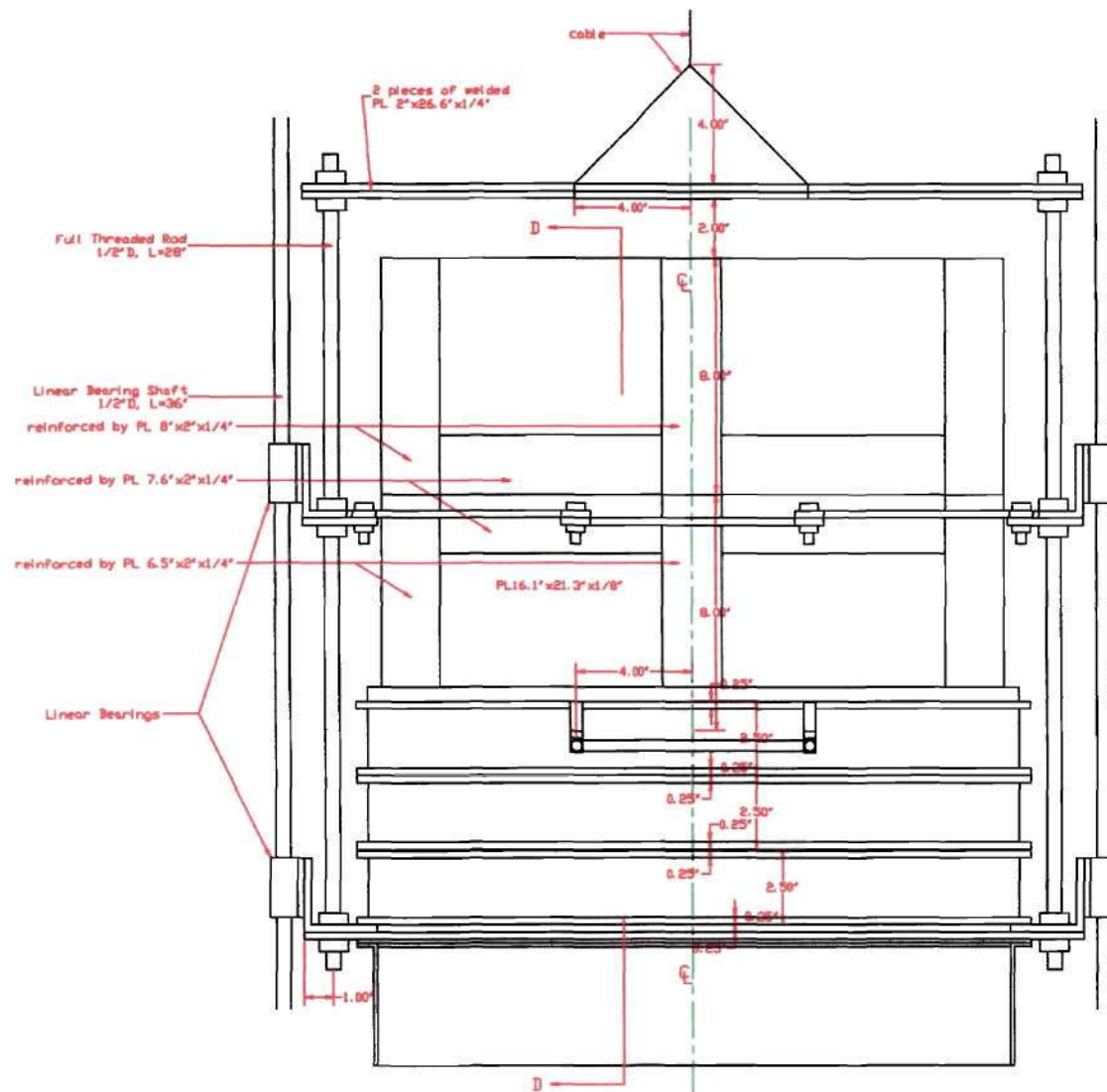
Ongoing Research

As noted earlier, additional research is ongoing even though the project is not funded by MAE/NSF. The scope of this additional research is to use quantitative image analysis based techniques to study the microstructure of sand within and outside the zones where sand blows occur. These experiments are utilizing techniques that have been developed by the investigators to study the inherent and induced microstructures in reconstituted triaxial specimens. Images captured from the surfaces of coupons cut from resin impregnated sand specimens are being quantitatively analyzed. Various metrics of the microstructure including local void ratio distributions and particle orientations are being examined. The previous tests conducted on reconstituted specimens have shown that parameters such as the entropy of the local void ratio distribution are strongly dependent on the structure of the material. A summary of the ongoing research program in slide format is provided in Figure 17. In combination with the observations summarized above, it is anticipated that a better understanding of the role of microstructure in the genesis/evolution of sand blows will be obtained.

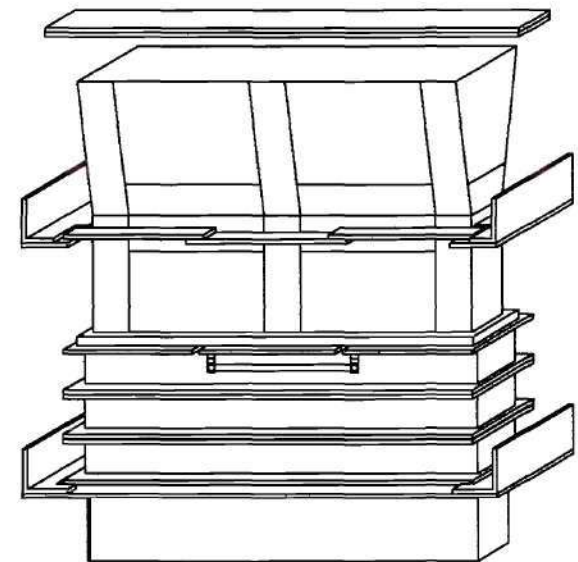


Pluviation System Frame Profile - FIGURE 1.

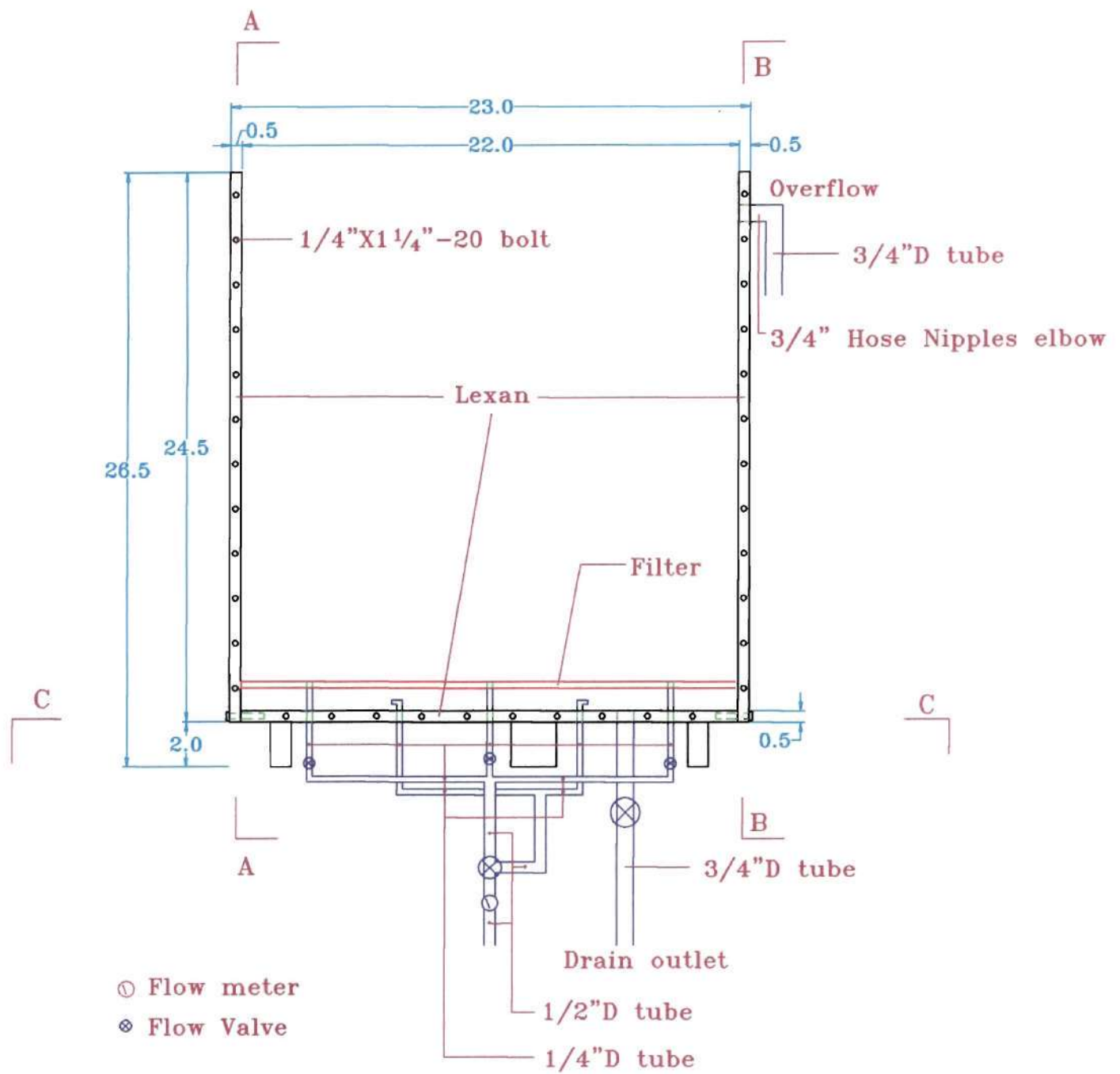




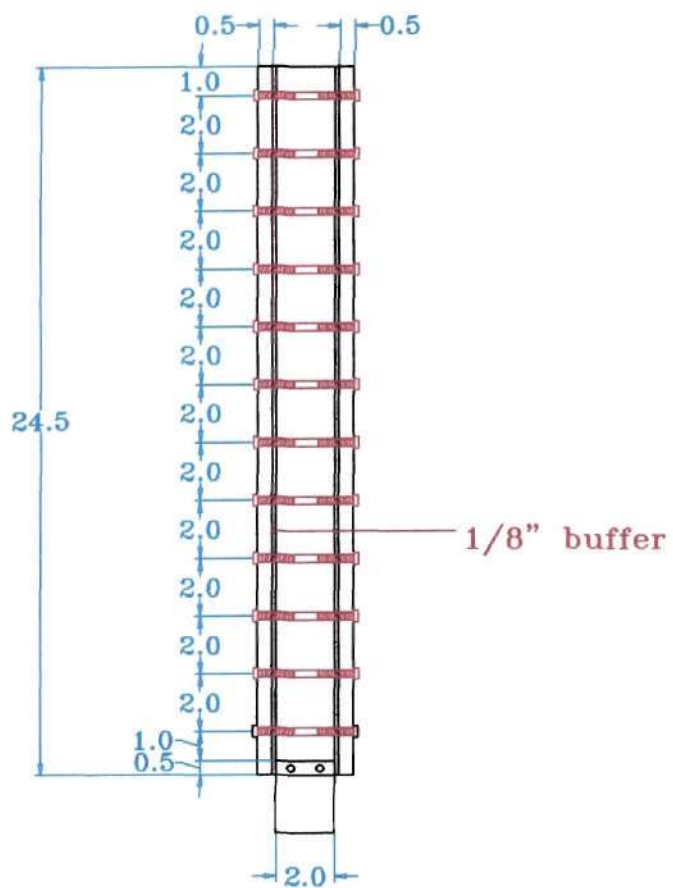
2-D Sand Tank Profile



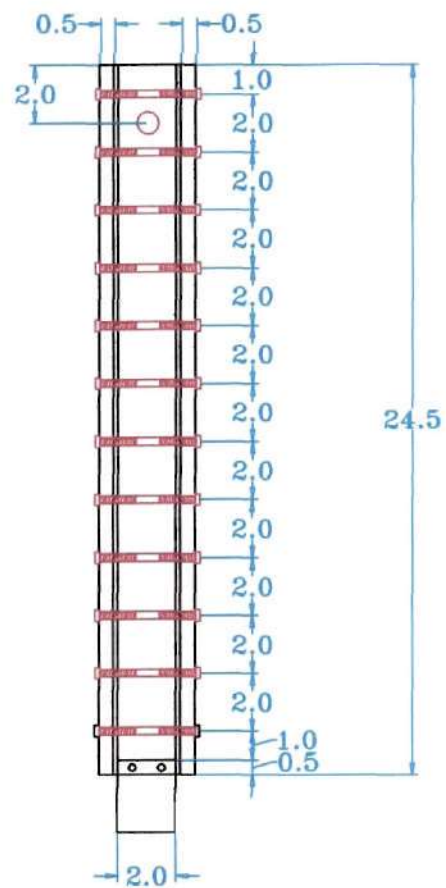
3-D Sand Tank Illustration



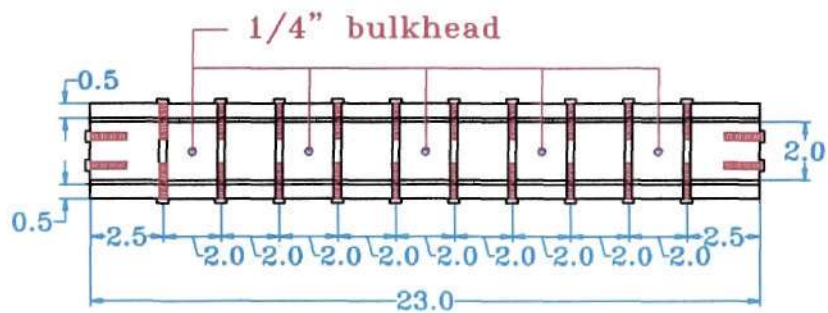
Configuration of Sandblow Tank- FIGURE 2.



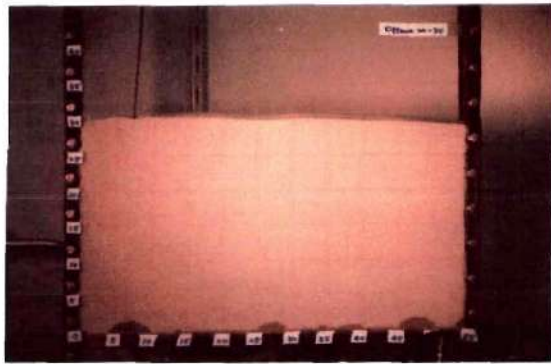
A-A section



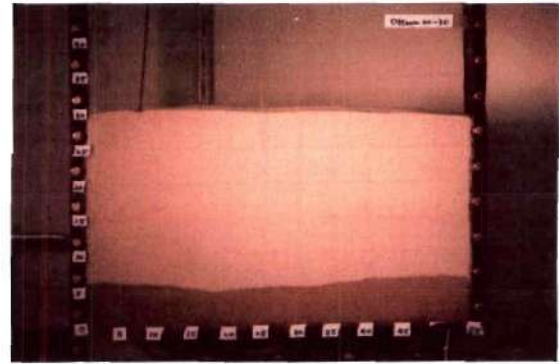
B-B Section



C-C Section



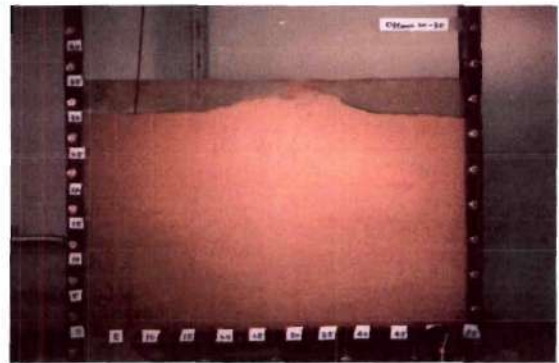
(a)



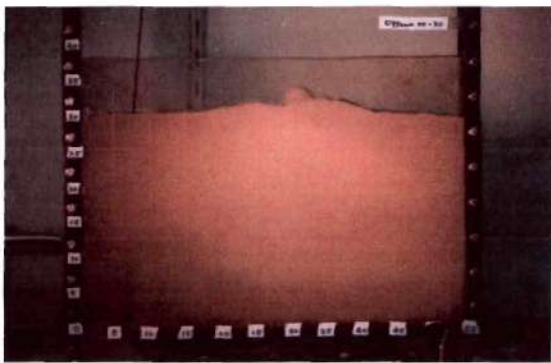
(b)



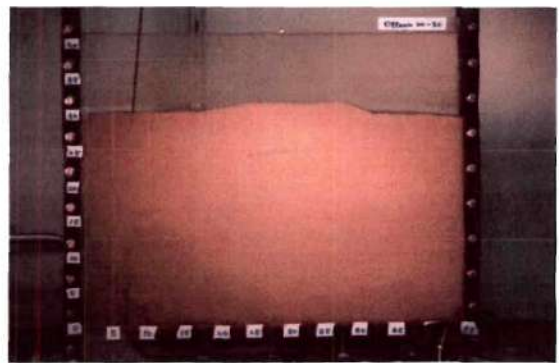
(c)



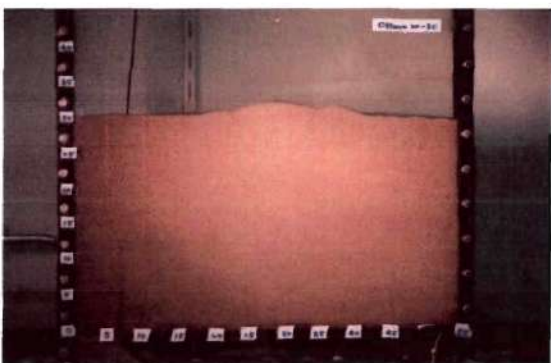
(d)



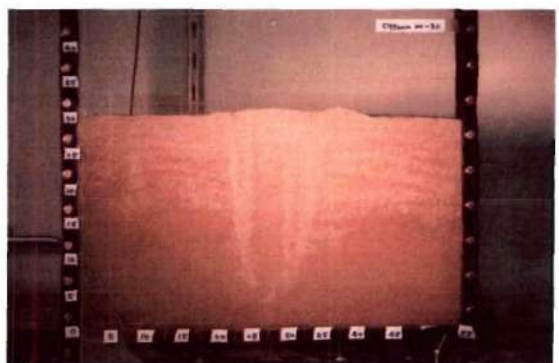
(e)



(f)

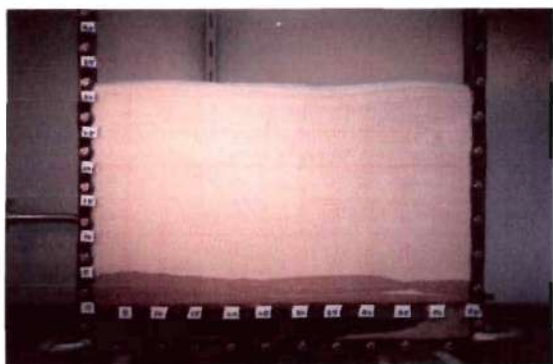


(g)

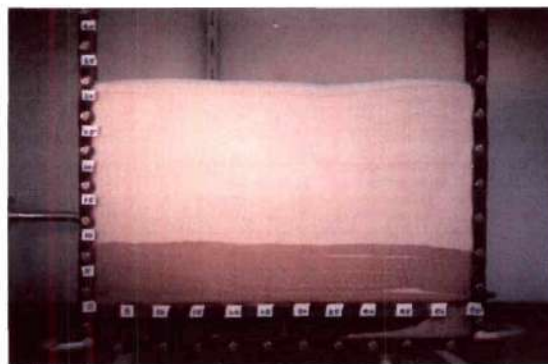


(h)

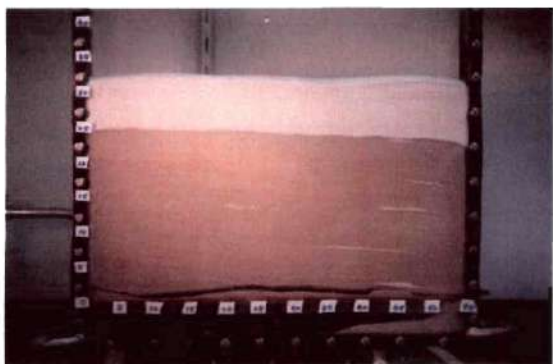
Figure 3: Sand blow in Ottawa 20-30 with artificial defect (homogenous flow)



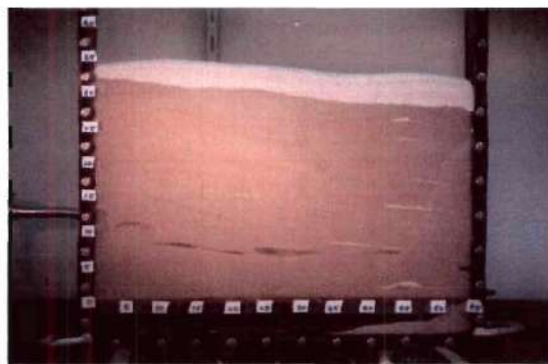
(a)



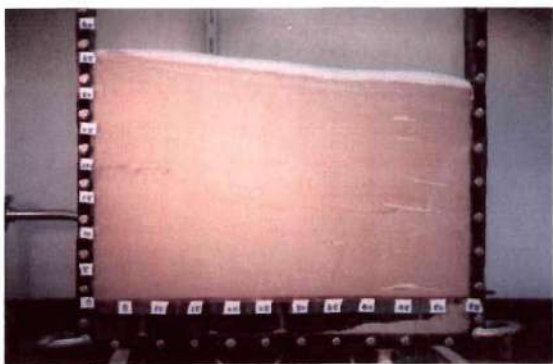
(b)



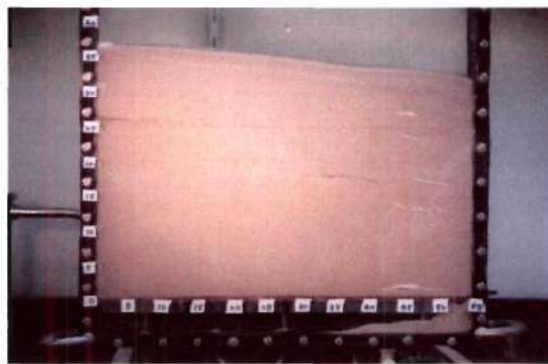
(c)



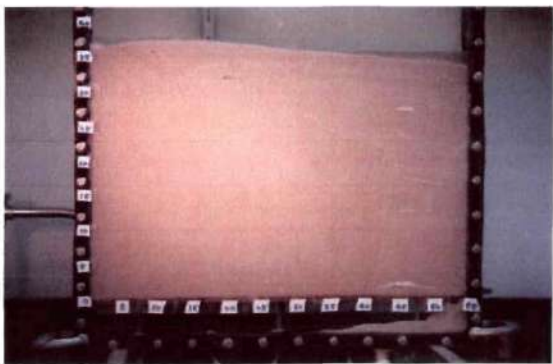
(d)



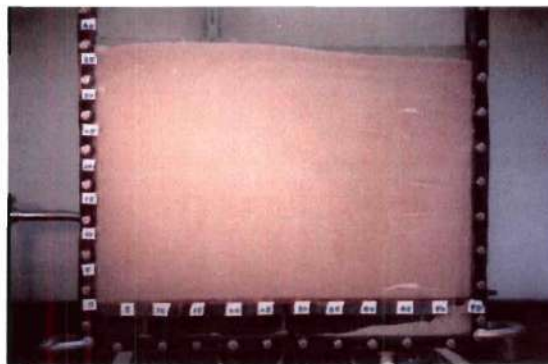
(e)



(f)

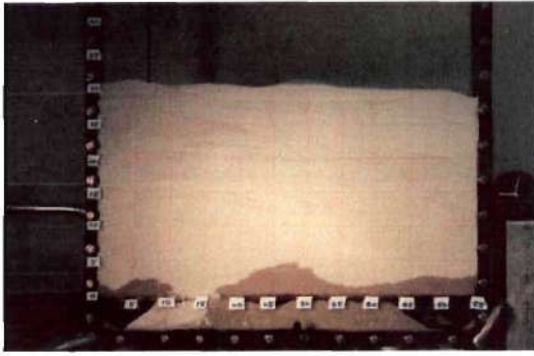


(g)

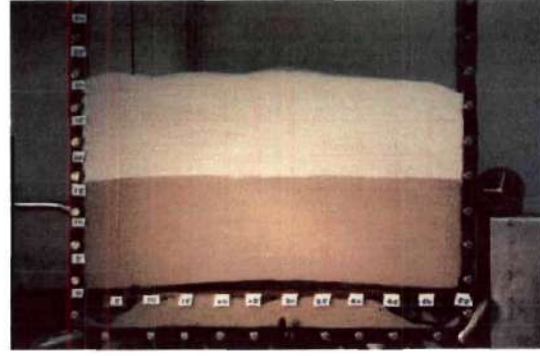


(h)

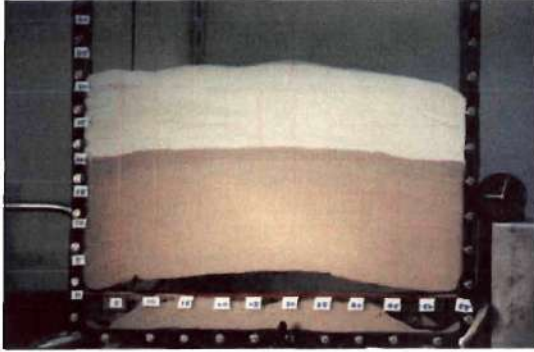
Figure 4: Sand blow in ASTM graded sand (homogenous flow)



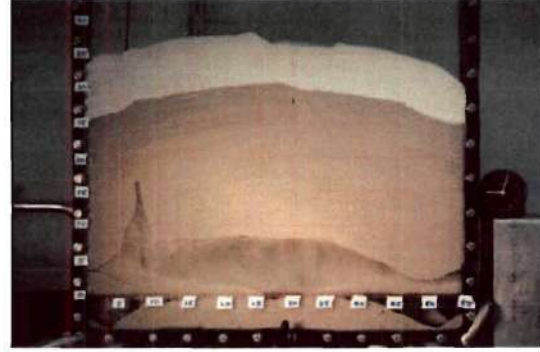
(a)



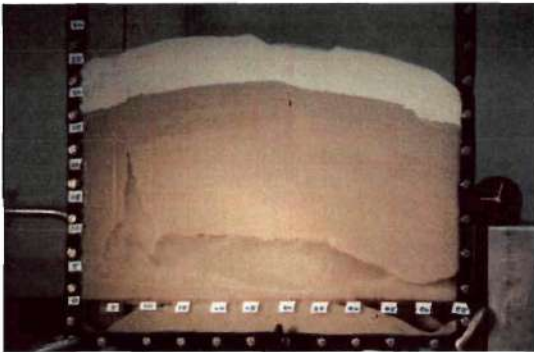
(b)



(c)



(d)



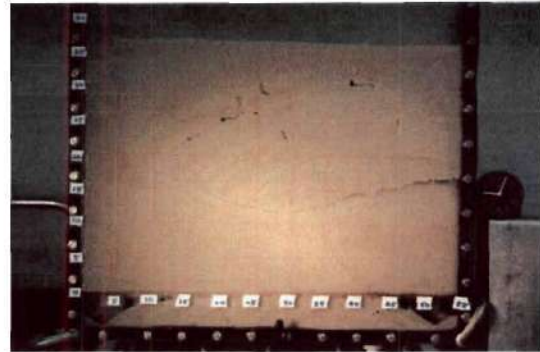
(e)



(f)

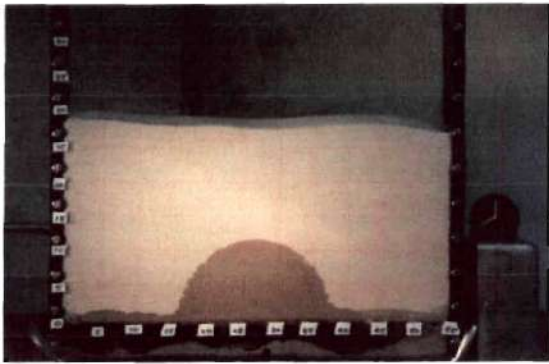


(g)

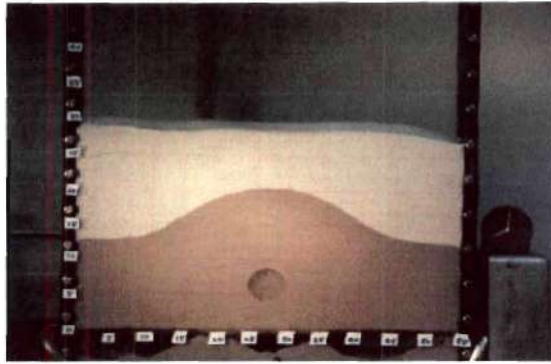


(h)

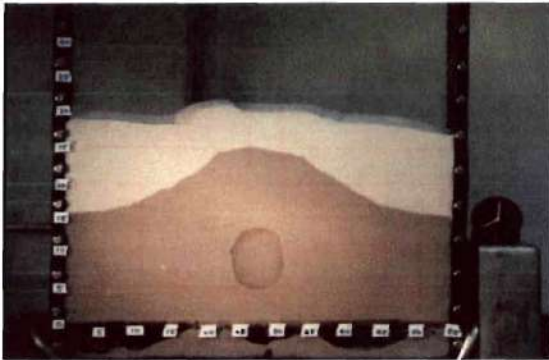
Figure 5: Sand blow in ASTM F-70 sand with artificial defect (homogenous flow)



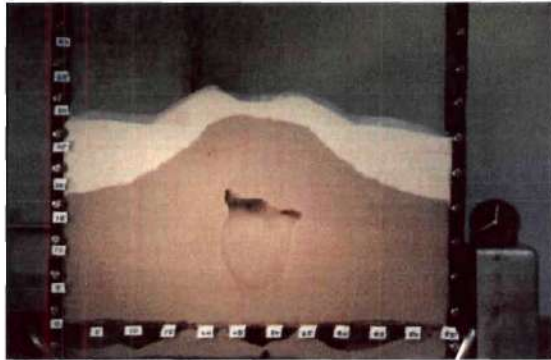
(a)



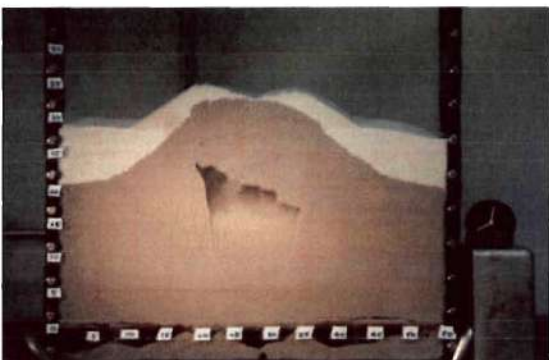
(b)



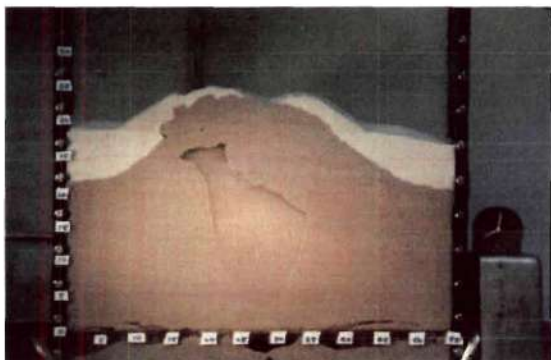
(c)



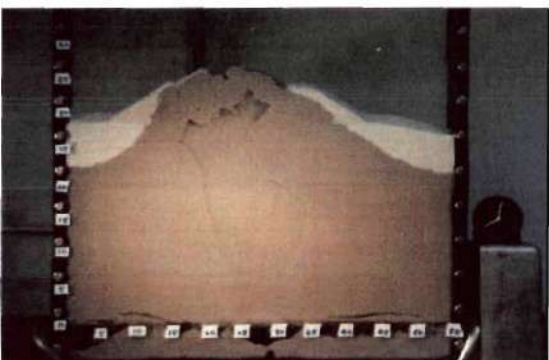
(d)



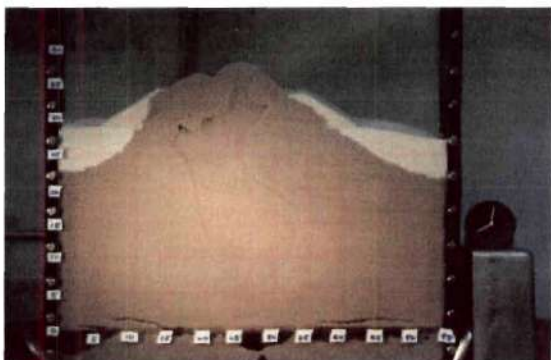
(e)



(f)



(g)

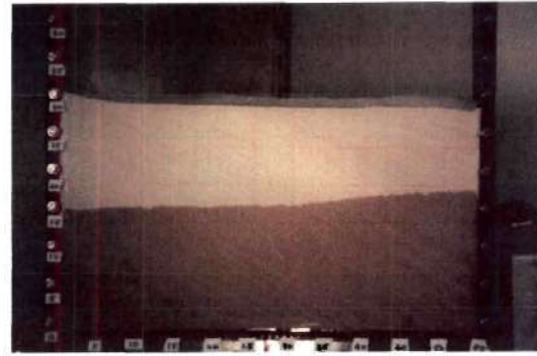


(h)

Figure 6: Sand blow in ASTM F-70 sand (concentrated flow)



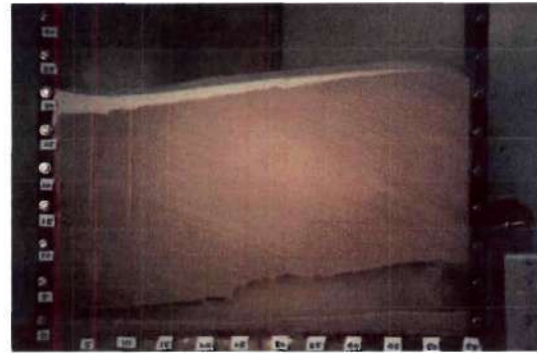
(a)



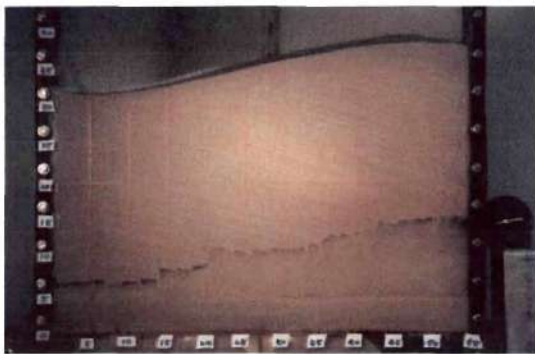
(b)



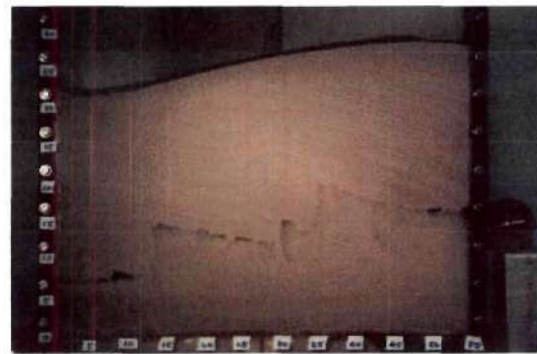
(c)



(d)



(e)



(f)

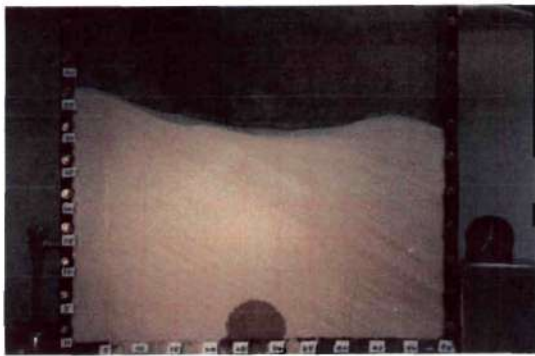


(g)

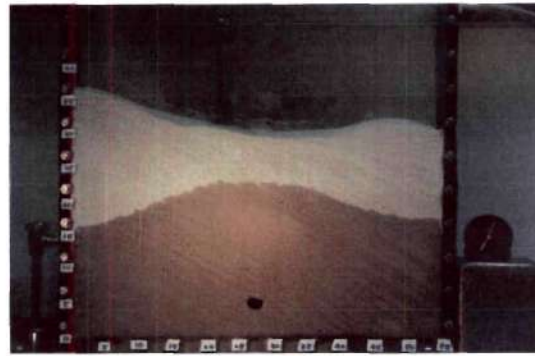


(h)

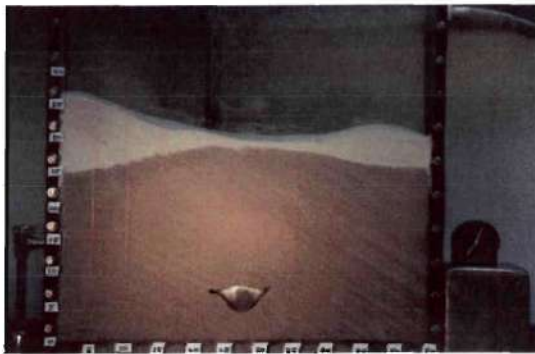
Figure 7: Sand blow in ASTM F-70 sand with inclined stratigraphy (homogenous flow)



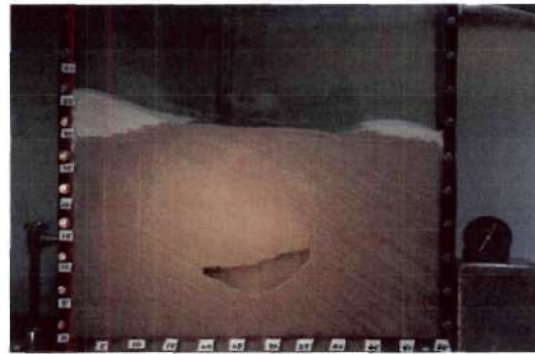
(a)



(b)



(c)



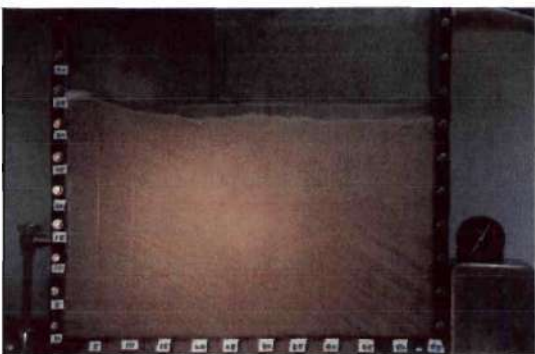
(d)



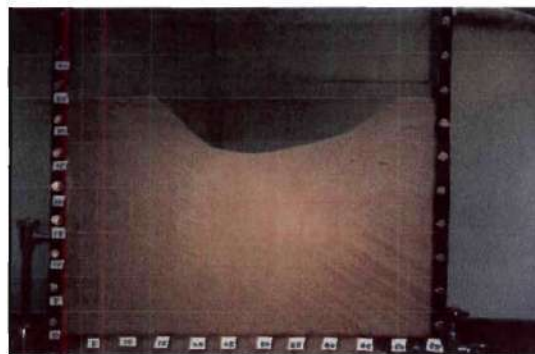
(e)



(f)

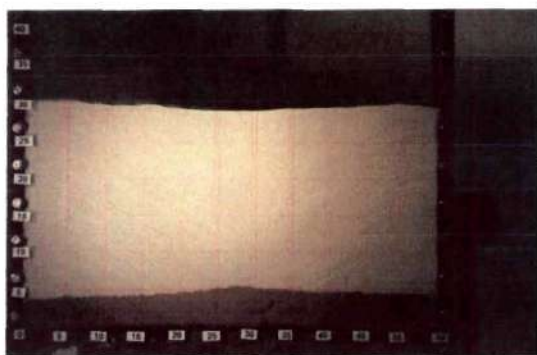


(g)

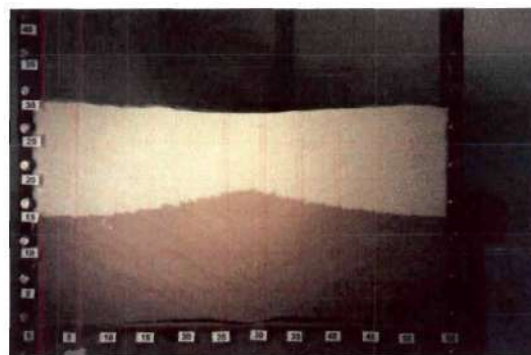


(h)

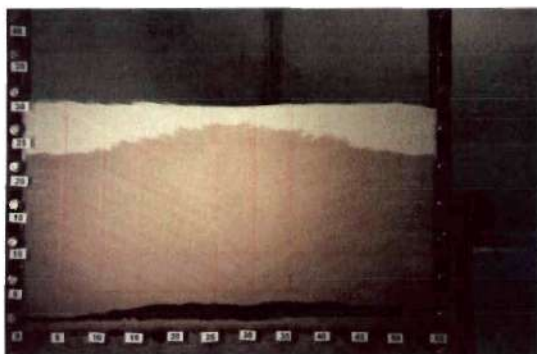
Figure 8: Sand blow in ASTM F-70 sand with inclined stratigraphy (concentrated flow)



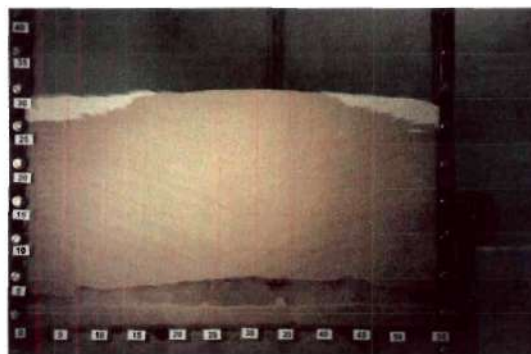
(a)



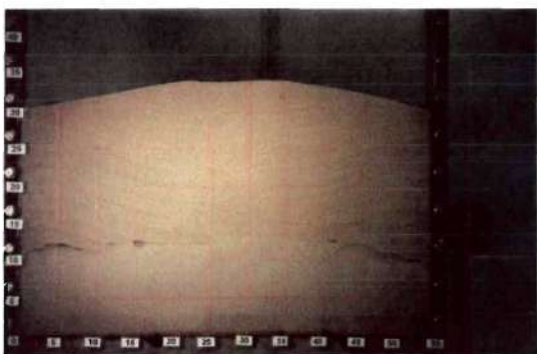
(b)



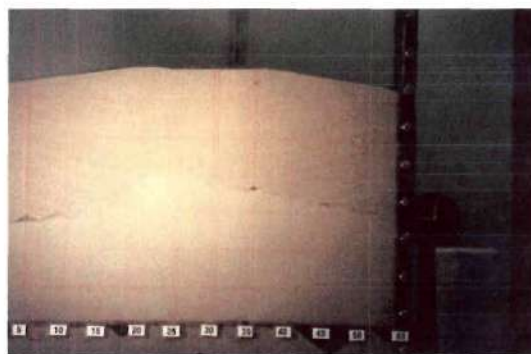
(c)



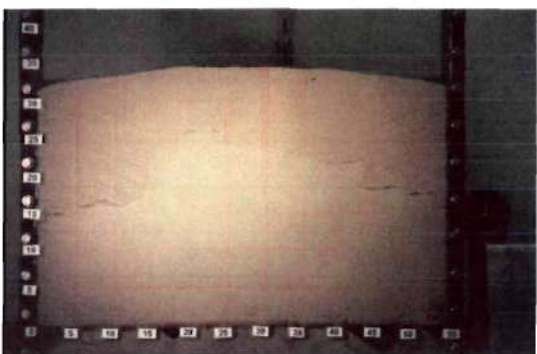
(d)



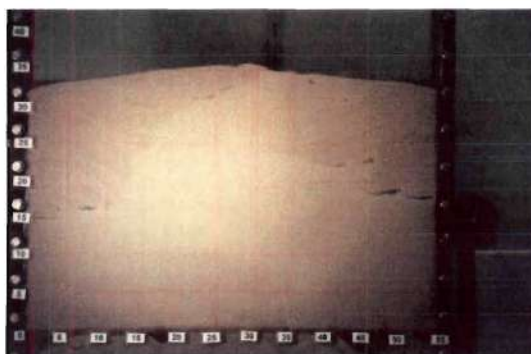
(e)



(f)

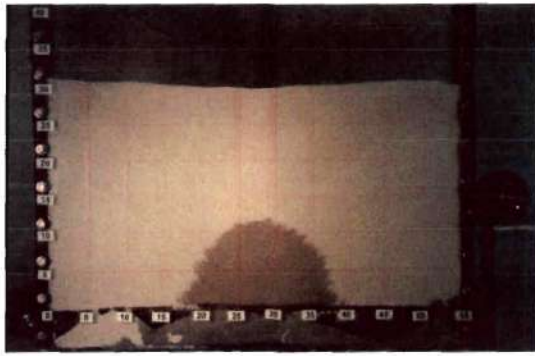


(g)

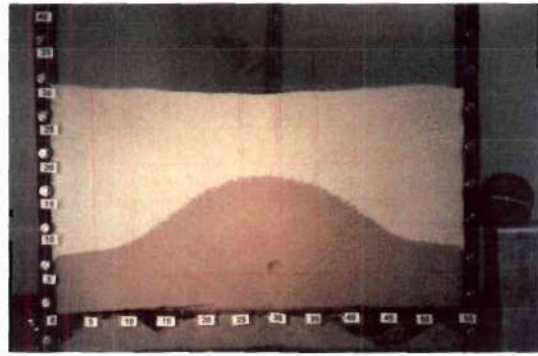


(h)

Figure 9: Sand blow in ASTM F-70 sand with synclinal stratigraphy (homogenous flow)



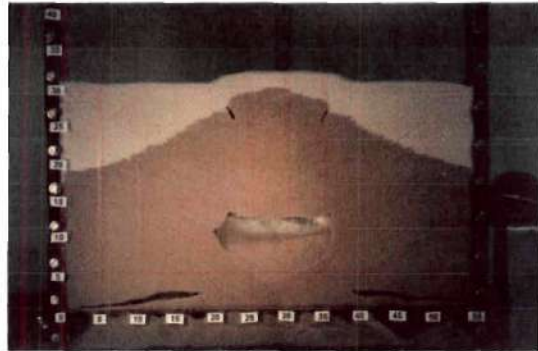
(a)



(b)



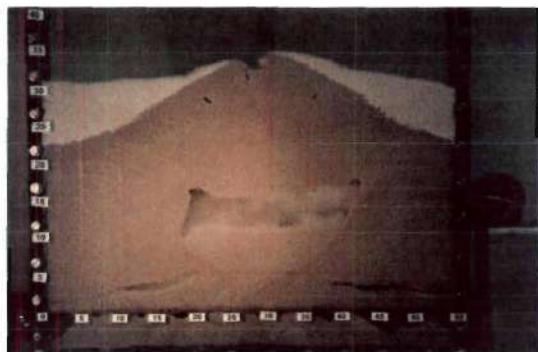
(c)



(d)



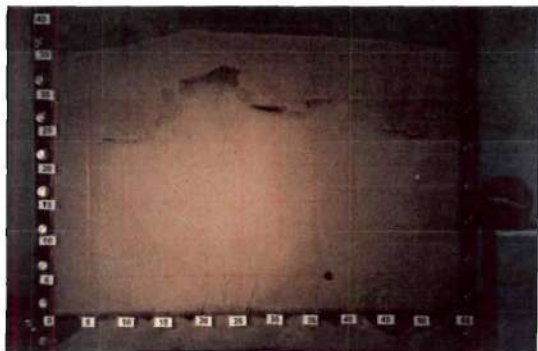
(e)



(f)

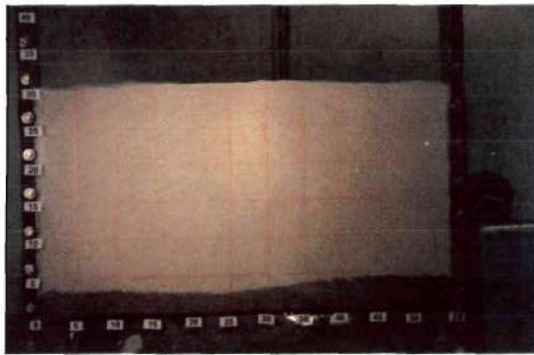


(g)

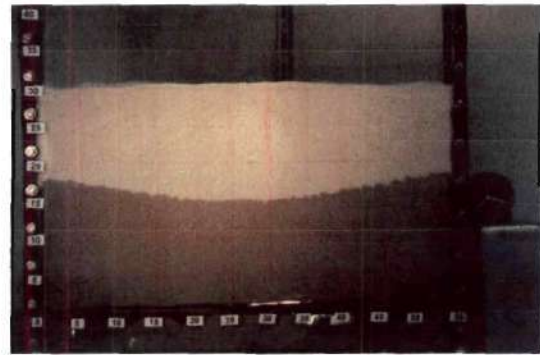


(h)

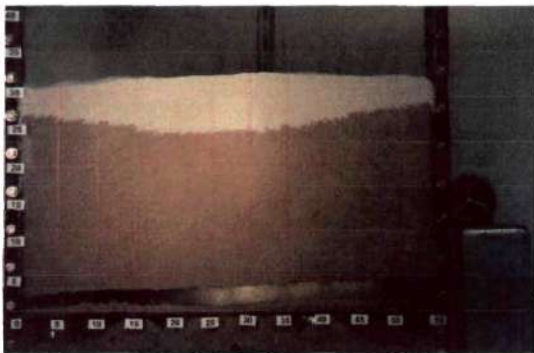
Figure 10: Sand blow in ASTM F-70 sand with synclinal stratigraphy (concentrated flow)



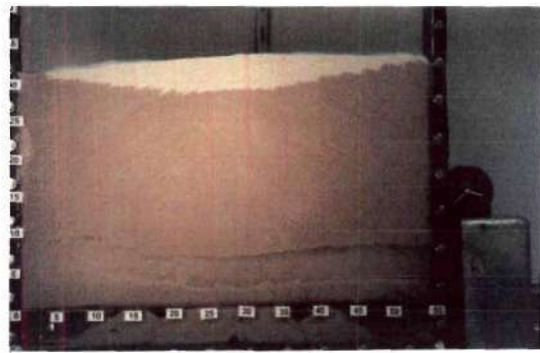
(a)



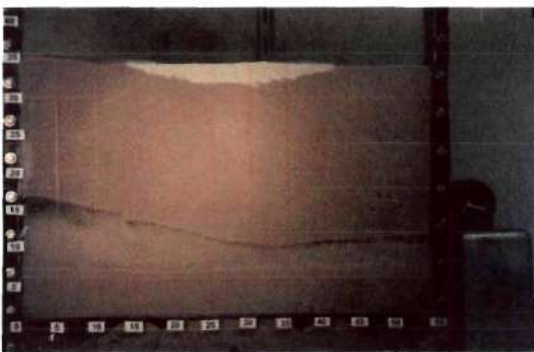
(b)



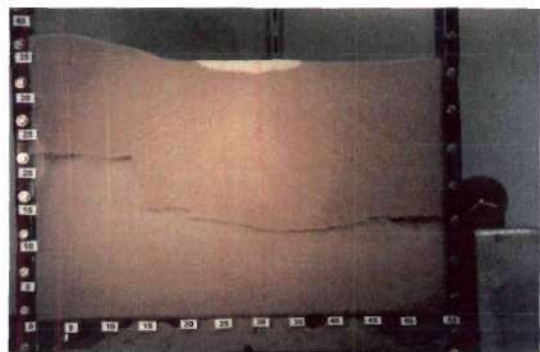
(c)



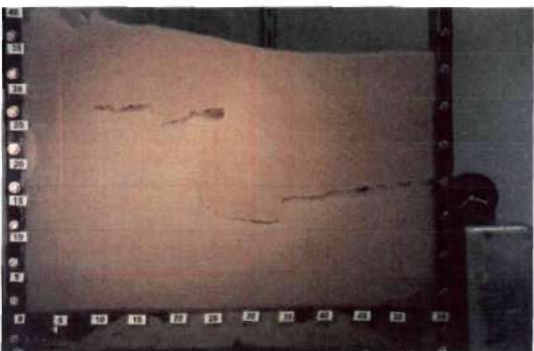
(d)



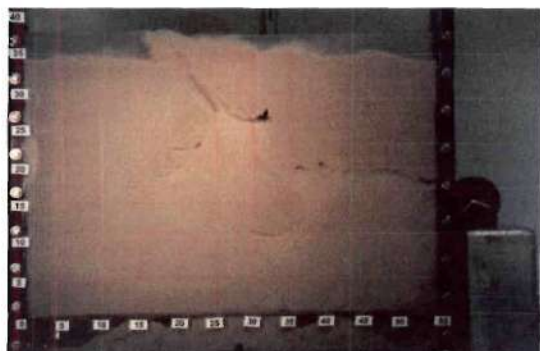
(e)



(f)

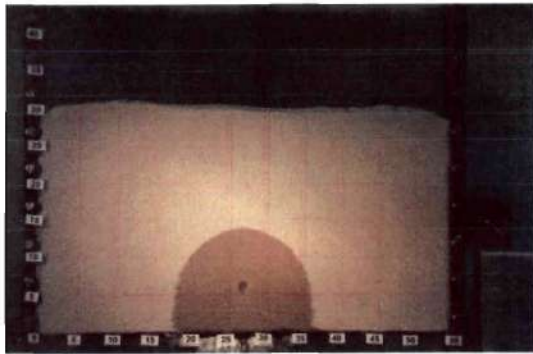


(g)



(h)

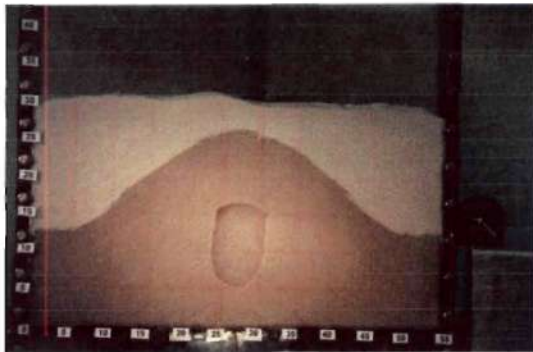
Figure 11: Sand blow in ASTM F-70 sand with anticlinal stratigraphy (homogenous flow)



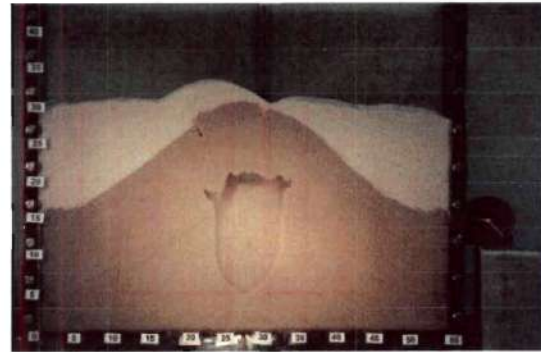
(a)



(b)



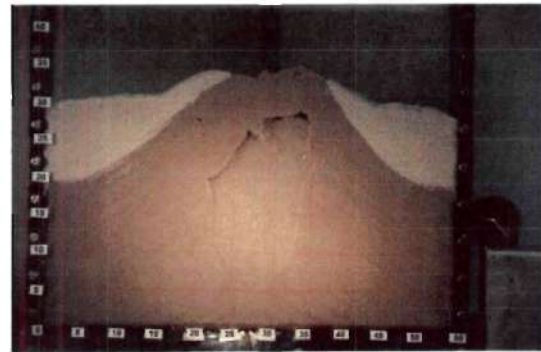
(c)



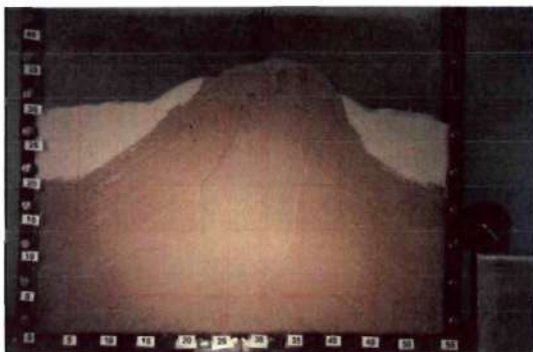
(d)



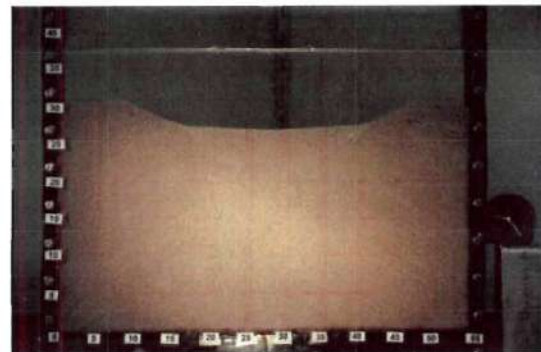
(e)



(f)

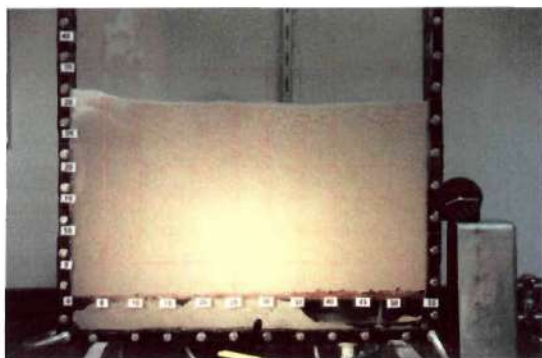


(g)

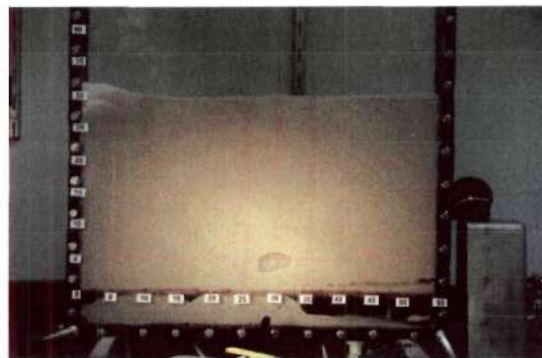


(h)

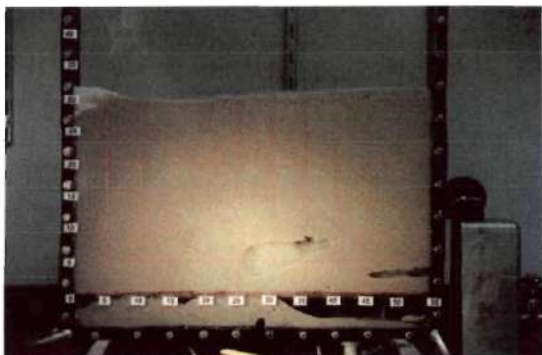
Figure 12: Sand blow in ASTM F-70 sand with anticlinal stratigraphy (concentrated flow)



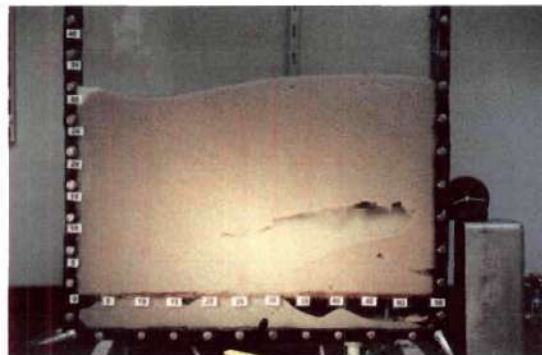
(a)



(b)



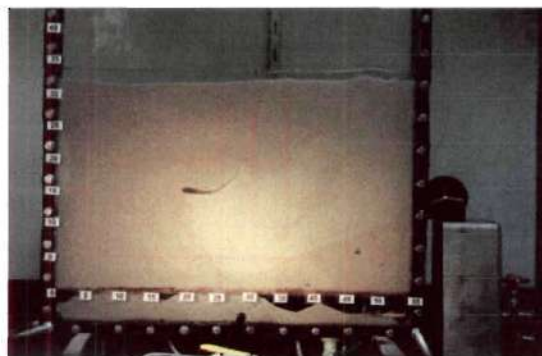
(c)



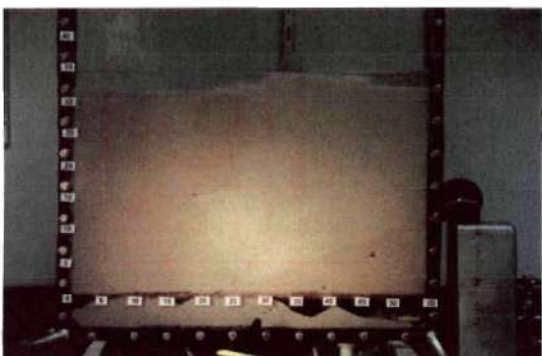
(d)



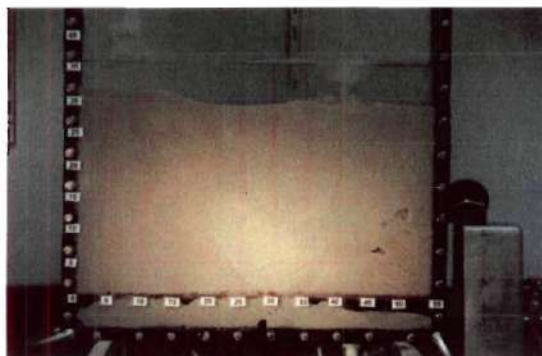
(e)



(f)

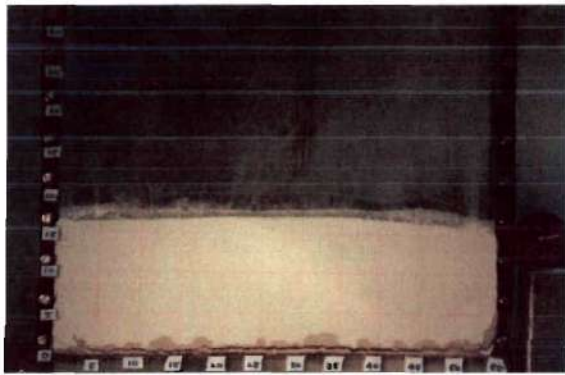


(g)

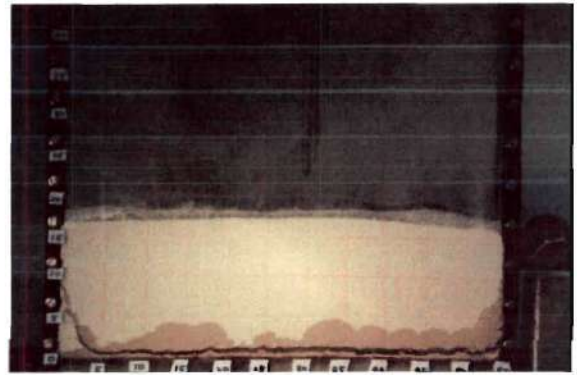


(h)

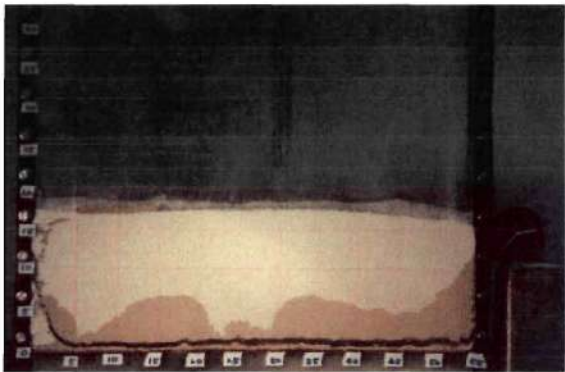
Figure 13: Sand blow in saturated ASTM F-70 sand with inclined stratigraphy
(concentrated flow)



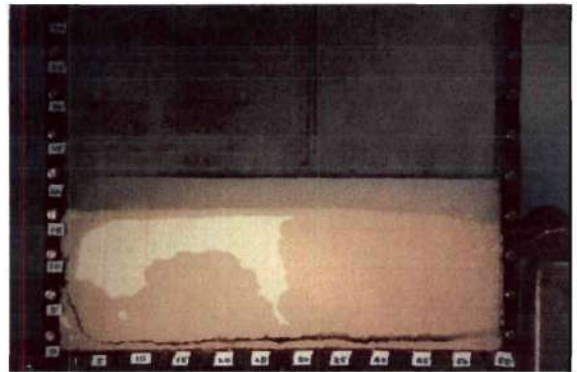
(a)



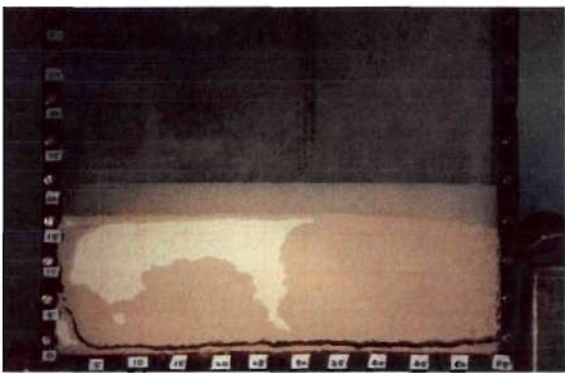
(b)



(c)

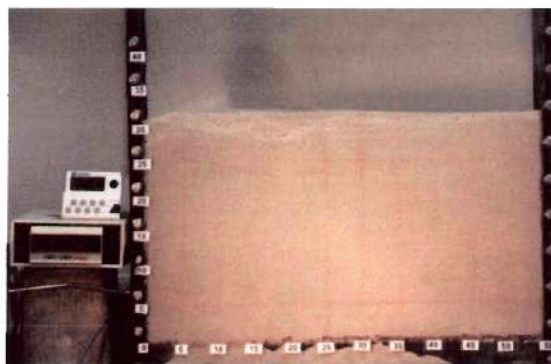


(d)

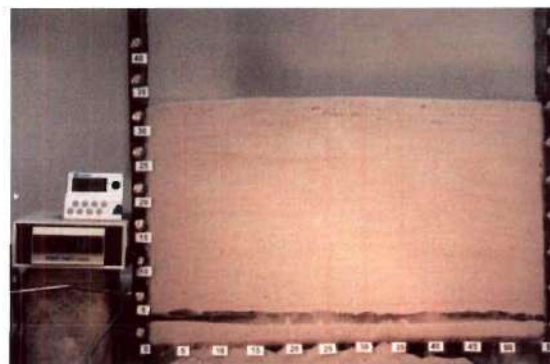


(e)

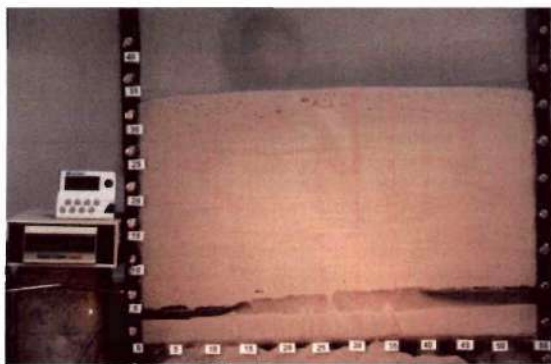
Figure 14: Blow in Kaolinite clay (homogenous flow)



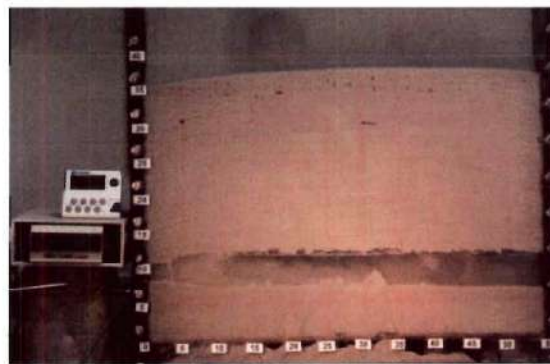
(a)



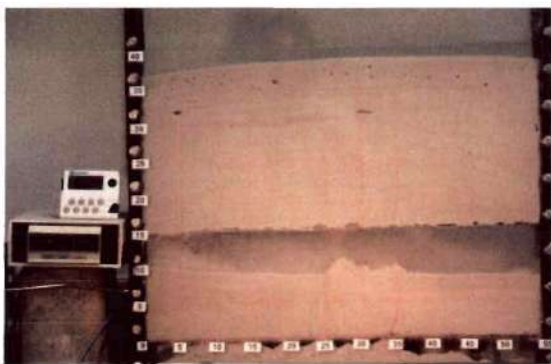
(b)



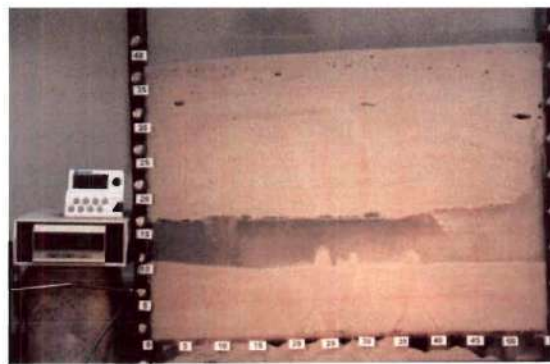
(c)



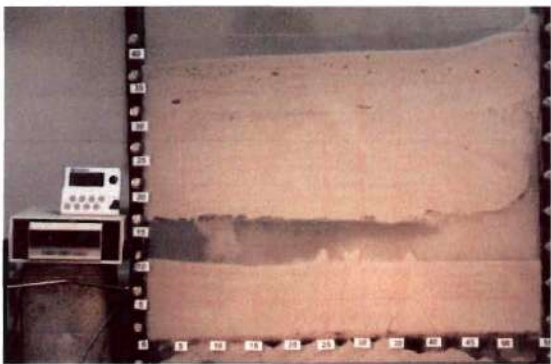
(d)



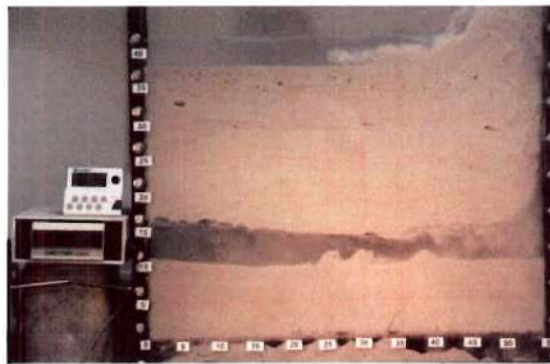
(e)



(f)

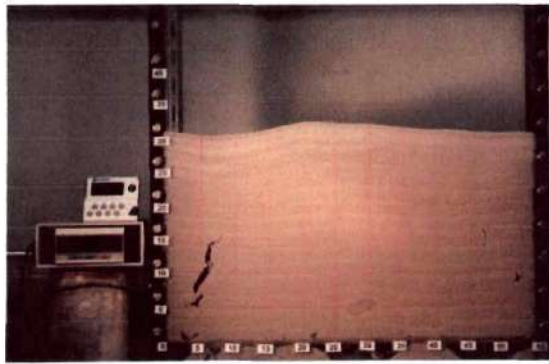


(g)

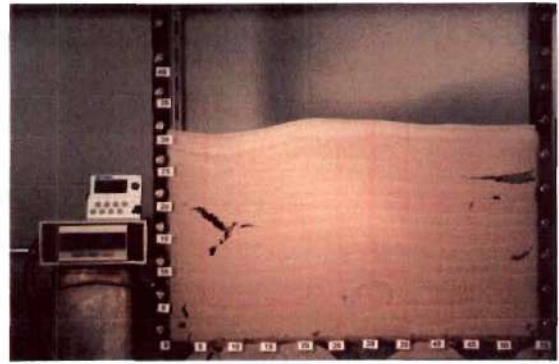


(h)

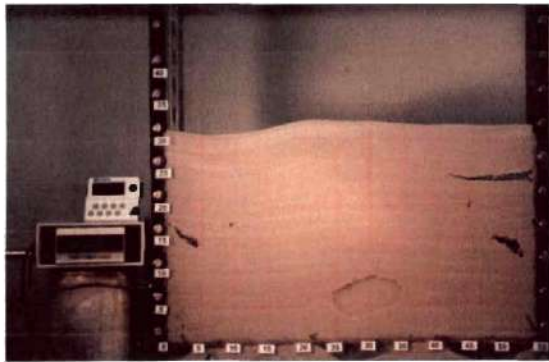
Figure 15: Sand blow in saturated ASTM F-70 sand (homogenous flow)



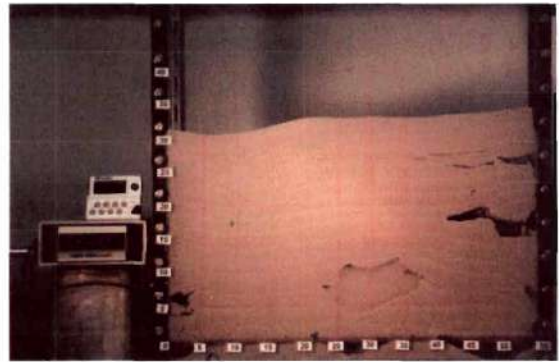
(a)



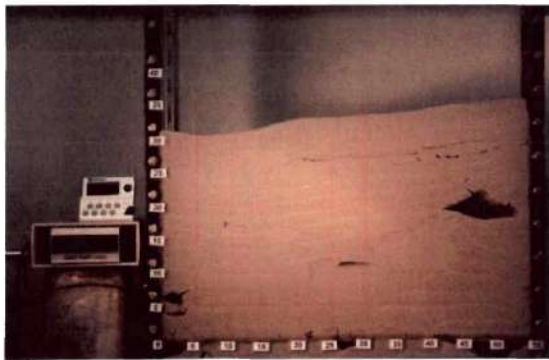
(b)



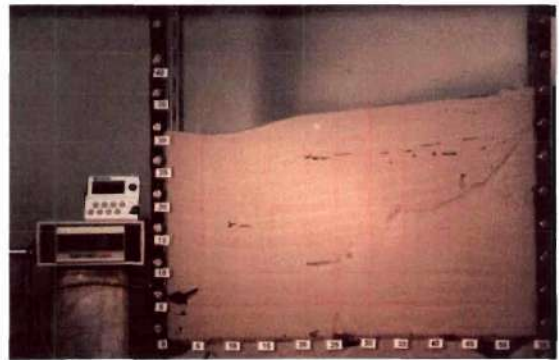
(c)



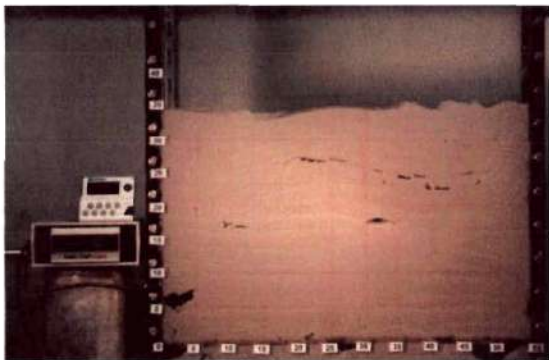
(d)



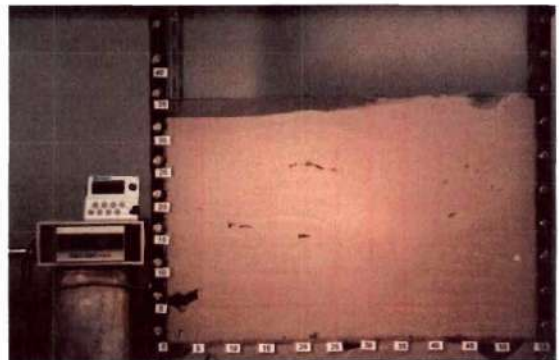
(e)



(f)



(g)

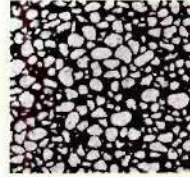


(h)

Figure 16: Sand blow in saturated ASTM F-70 sand (concentrated flow)

Microstructure Effects from Sand Blows

- Focus of sub-study is to quantitatively examine sand microstructure relationship to sand blow occurrence



- Image analysis based techniques are being used to study pre- and post-blow sand microstructures
- Same techniques have been successfully used to study differences in initial and evolving sand microstructure due to different laboratory reconstitution methods

Microstructure Effects from Sand Blows

- Microstructure of sand in a 2-D tank before a sand blow is induced is quantitatively evaluated



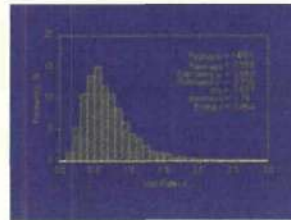
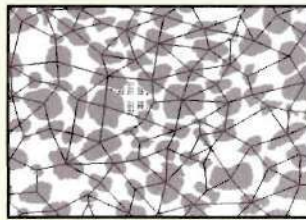
- Microstructure in same tank after a sand blow is induced is quantitatively evaluated



FIGURE 17.

Microstructure Effects from Sand Blows

- Surfaces of coupons cut from resin impregnated specimens are prepared using differential pressure polishing
- Brightfield microscopy is used to capture images
- Metrics of microstructure (local void ratio, particle orientations) are automatically quantified



Microstructure Effects from Sand Blows

